

Pore Surface Fractal Dimension of Sol-gel Derived Nano-porous Silica-zirconia Unsupported Membrane

Maryam Shojaie Bahaabad^{1,*}

¹ Department of Chemical and Materials Engineering, Shahrood University of Technology, Shahrood, Iran

ARTICLE INFO

Article history:

Received 3 October 2016

Accepted 15 November 2016

Available online 25 December 2016

Keywords:

Ceramic membrane

Pore structure

Surface fractal dimension

Sol-gel

ABSTRACT

Pore surface roughness changes in SiO₂-ZrO₂ unsupported membranes induced by chemical composition and heating process have been investigated by the analysis of surface fractal dimension. Fractal features were analyzed from N₂ adsorption-desorption measurements. It was found that a decrease in the surface fractal dimension occurs while the zirconia content increases in the unsupported membranes heated at 500 °C. The surface fractal dimension of membrane with 30 mol% silica content slightly increased in the heating range of 200 to 500 °C due to the shrinkage and increase of mass fractal dimension of silica clusters.

1. Introduction

Recently, ceramic membranes have received considerable attention due to their applications in chemical, petrochemical and drug and food industries where high temperature and high pressure is needed. Physical and chemical structures of ceramic membranes are determinant factors in various key properties such as permeability, selectivity, thermal, hydrothermal stability and fouling manner. In the sol-gel method, synthesis of the gel is based on hydrolysis and condensation reactions to form oxide network from molecular precursors through making chemical bandings [1-6].

Among competing membranes, sol-gel derived silica-based membranes are the most attractive because of their amorphous structure and pore sizes less than 1 nm and also relatively low cost of production. Micro-porous SiO₂ membrane is usually used for gas separation involving small gas molecules such as H₂, He, N₂, CO₂, CH₄, etc. because of excellent selectivity and high gas permeation. Micro-porous amorphous silica based membranes are

well known for their H₂ permselectivity [7-11] and the only drawback of the silica membrane application is its poor hydrothermal stability when exposed to water and water vapor at high temperatures [12-14].

In order to improve the silica membrane hydrothermal stability, many oxides and metal ions addition such as NiO, TiO₂, ZrO₂, Cr₂O₃, Co₃O₄, Al₂O₃, Nb₂O₅, etc. have been investigated [15-21]. The characterization of pore structure, which determines the permeation process of membrane, is of great importance. So far, most investigations have focused on such pore structure as specific surface area and pore size distribution, but the surface fractal, the important parameter reflecting the roughness of pore surface, has drawn little attention. It is obvious that the surface area and pore size distribution alone do not meet all requirements to describe the characteristics of the pore structure of a membrane [22, 23]. In order to determine the pore size distribution of membranes, it is often essential to make assumptions about the pore geometry.

* Corresponding author:

E-mail: mshojaieb@shahroodut.ac.ir

One of the idealized pore structures is parallel non-intersecting cylindrical pores, the surface of which is assumed to be smooth and the details are not taken into account. In the actual case, the formation of pore structures, either by the packing of particles or by interpenetration of inorganic polymeric clusters, results in irregular pore surface. Surface fractal dimension, D , ranging from $D=2$, for perfectly smooth surfaces, to $D=3$, for sponge-like surfaces, can be used to describe the irregularities and roughness of pore surface at the atomic or molecular level [24 – 26]. The magnitude of the surface fractal dimension of membranes has great influence on such important physicochemical processes as adsorption, surface diffusion, and catalysis. Nevertheless, it is still an ambiguous problem to measure the value of D , which may vary according to the methods used. In this study, a method proposed by Avnir and Jaroniec [27] is performed to determine surface fractal dimensions from a single adsorption isotherm. In accordance with Avnir and Jaroniec, the surface fractal dimension can be obtained by extending the Frenkel – Halsey – Hill (FHH) model for multilayer adsorption, yielding the following equation:

$$N/N_m = k [\ln (P/P_0)]^{D-3} \quad (1)$$

where N/N_m is the number of layers adsorbed on the surface, k is a constant, and P and P_0 are the equilibrium and saturation pressure of nitrogen adsorbed, respectively. FHH equation provides a relationship between the surface fractal dimension and nitrogen adsorption, that is to say, the pore surface roughness can be probed by nitrogen molecules.

The value N_m can be obtained from the BET model, and the surface fractal dimension can be calculated from the slope of a plot of $\ln (N/N_m)$ vs. $\ln [\ln (P_0/P)]$. Using the fractal analysis approach, the present paper aims to determine the surface roughness of the unsupported SiO_2 - ZrO_2 membranes, and to study the effect of $\text{ZrO}_2/\text{SiO}_2$ molar ratio and temperature on the surface fractal dimension.

2. Materials and methods

2.1. Sol preparation

A polymeric SiO_2 - ZrO_2 sol was produced starting from tetraethyl orthosilicate (TEOS,

Merck Co., Germany), zirconium isopropoxide (ZIP, Fluka), 2-methoxy-4-propenylphenol (isoH, Merck Co., Germany), nitric acid (65%, Merck Co., Germany) and ethanol (EtOH, Merck Co., Germany). The procedure of sol preparation is shown in Figure 1. The molar ratio $\text{TEOS}:\text{EtOH}:\text{H}_2\text{O}:\text{HNO}_3$ was 1:3.8:1:0.06 in SiO_2 sol. For preparation of ZrO_2 sol, the molar ratio isoH/Zr, isoH/EtOH and Zr/EtOH was 2, 0.1, and 0.02, respectively. Molar ratio of $\text{ZrO}_2/\text{SiO}_2$ was 0, 30 and 50 in the sols. The resultant sols were dried as xerogel powders (unsupported membrane) by drying the coating sol in petri dish. Afterwards, they were dried for 72 h in ambient temperature with 80% humidity. The samples were heat treated at 500 °C for 1 h.

2.2. Characterization

A Dynamic Light Scattering Analyzer (DLS, Malvern, ZEN3600) was used to measure the particle size distribution of the sols. DLS measurement determines the velocity at which the particles within a solvent diffuse due to Brownian motion. This is done by monitoring the fluctuations of intensity of the scattered light beam over time.

The scattered intensity varies constantly depending on the particle size due to phase addition of the moving particles. The Brownian diffusion velocity is inversely proportional to the particle size and is expressed as hydrodynamic radius R_H according to the Einstein equation:

$$R_H = 2kT/3D \quad (2)$$

where D is the translational diffusion coefficient, k is the Boltzmann constant, T is the absolute temperature and corresponds to the solvent viscosity.

Unsupported membrane structural properties were characterized by Fourier Transform Infrared (FTIR) to determine the bonds. FTIR was carried out using a Perkin – Elmer Spectrum with the range of 400–4000 cm^{-1} . Pore size distribution, pore volume and surface area of unsupported membrane were measured by N_2 adsorption–desorption (BET, Micrometrics Tristar 3020) analysis. The characterizations were carried out on unsupported membranes by assuming that their properties are similar to those of supported membrane layers.

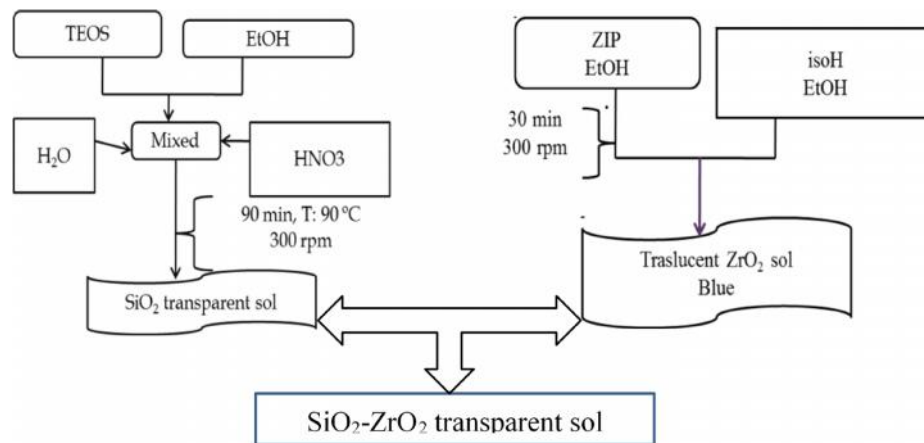


Fig. 1. Schematic of preparation of SiO_2 - ZrO_2 polymeric sol.

3-Result and discussion

3-1- characterization of unsupported membrane

3-1-1- DLS

Particle size distribution of the prepared polymeric silica sol containing 0, 30 and 50 %mol zirconia measured by DLS is shown in Fig. 2. For the sol-gel derived membranes, the pore sizes are determined by the primary particle size distribution in the sol [28]. For the polymeric sol, under controlled conditions, hydrolysis and condensation reactions lead to the formation of three-dimensional network of branched polymers. The structure of the pores

created in the coated layer by polymeric sol will depend on the structure of these individual clusters [29]. For the prepared samples the particle sizes are in the range of 0.6–2.2 nm, which are considered as hydrodynamic diameters of these non-spherical particles. These sols are therefore potentially suitable precursors for making micro-porous thin layers. Smaller hydrodynamic diameter can be regarded as low branched silica polymers. Low branched silica species can interpenetrate into each other leading to a micro-porous network due to a highly compacted material. On the other hand, highly branched clusters are not able to interpenetrate due to steric hindrance [29].

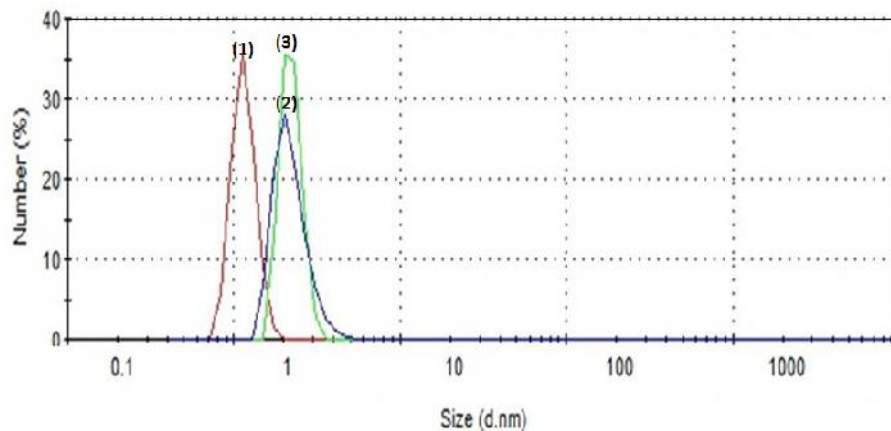


Fig. 2. Particle size distribution of SiO_2 sol with different amount of zirconia (1) 0, (2) 30% and (3) 50%.

The particle size increased with the increasing of ZrO_2 in the sol. Electronegativity of $Zr(OE)_4$ (0.65) is higher than $Si(OE)_4$ (0.32) [30, 31]. Thus, zirconium has duplex silicon electropositive charge, which explains why the hydrolysis and condensation rate of zirconium alkoxide is much faster than TEOS. Therefore, zirconium consumes water and then silica sol is concentrated.

Concentrated solutions cause agglomeration and particle size growth. According to the similar works done upon silica layer, increasing water in the sol leads to the decrease of the pores size, which is affected by the fine sol particles [32]. Also, the addition of zirconium into the solution causes the increase in the pH from 2.27 to 5.55 due to the basic nature of the zirconium solution [33]. At higher pH, low branched silica clusters appear which are not inevitable to make micro-porous structure. As a result, increasing zirconium in the silica sol makes the sol particles coarse.

3-1-2- FT-IR

In this study, in order to synthesize the silica membrane with hydrothermal stability, chemical bandings of the mixed oxides were investigated using FTIR analysis. Figure 3 shows the FTIR spectra of the unsupported 0, 30% and 50% zirconia doped silica membranes heat treated at 500 °C.

The absorption bands at 3735 cm^{-1} and 2336 cm^{-1} are due to O–H stretching vibration in water, alcohol molecules and silanol groups (Si–OH).

The peaks at 1643 cm^{-1} and 1504 cm^{-1} are related to bending vibrations of water molecules and CH₂ and CH₃ groups. The absorbed bands at about 1079 cm^{-1} corresponds to siloxane (Si–O–Si) asymmetric [34].

The band at 802 cm^{-1} is usually coupled with the hint of tetrahedral coordination of Zr^{+4} ions which should substitute for Si^{+4} (Si–O–Zr) [34]. The band at 740 cm^{-1} could be due to the existence of Si–O–Zr bonding [35]. The reaction mechanism for this sol–gel system can be explained as follows: the first step is TEOS hydrolysis to Si–OH and subsequently condensation of these groups to form Si–O–Si chains. Interaction between silicon and zirconium ion can happen in this way: polymeric molecules of $Si(OH)_4$ can absorb Zr^{+4} ions from solution and these ions can break the formed Si–O–Si bonds and cause Si–O–Zr formation [36]. By continuing this process and distributing Si–O–Zr all over silica structure, homogenous silica-zirconia polymeric network is formed. The peaks corresponding to these bands have higher intensity for the samples with 50% zirconia compared with one containing 30% zirconia. More zirconium ions are incorporated into the silica network as the concentration of zirconia increases in the sol and cause more Si–O–Zr linkages formation.

The XRD patterns of the silica-zirconia xerogel with different amounts of zirconia calcined at 500 °C for 1 h are shown in Figure 4. As the XRD measurements demonstrate, unsupported membranes are kept amorphous after calcination at 500 °C.

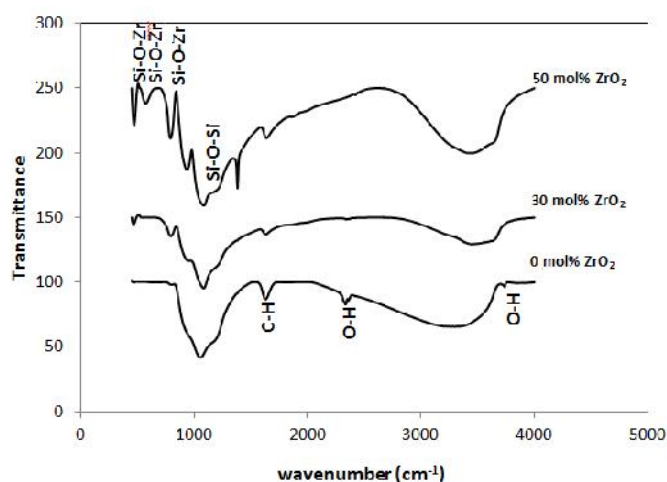


Fig. 3. FTIR spectra of silica containing 0, 30% and 50% zirconia xerogel heat treated at 500 °C for 1 h.

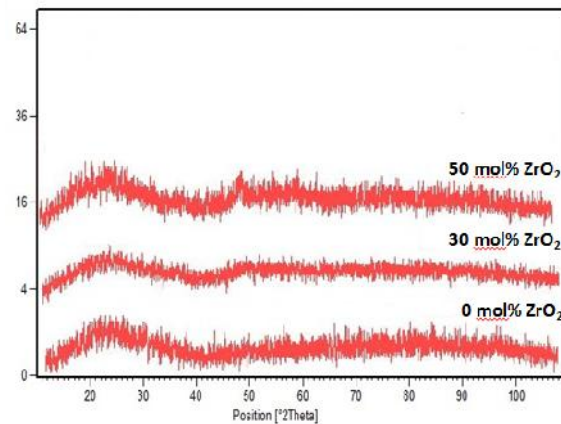


Fig. 4. XRD pattern of SiO₂-ZrO₂ xerogel heat treated at 500 °C for 1 h.

3-1-3- BET

The BET analysis is the standard method to determine the surface area from nitrogen adsorption isotherms. Fig. 5 exhibits the adsorption–desorption isotherm and pore size distribution of unsupported silica-zirconia membranes calcined at 500 °C for 1 h. Fig. 5 demonstrates the coincidence of desorption isotherm with adsorption isotherm and the absence of hysteresis loop for silica unsupported membrane. Consequently, the curve corresponds to the I-type adsorption isotherm, suggesting micro-porous structure of the sample.

The isotherms of unsupported silica-zirconia membranes with 30% and 50% zirconia are closely consistent with those classified as type IV adsorption isotherm and the presence of the hysteresis loops confirms that meso-pore does exist in these samples.

The adsorption data are plotted according to Eq. (1) and the results are illustrated in Figure 6. The plots are not linear over the entire isotherm, exhibiting curvature below monolayer coverage and beyond coverage values where capillary condensation occurs. Since the FHH equation is accurate only for multilayer adsorption, the D values obtained from sub-monolayer region and capillary condensation region of the isotherms prove to be highly unrealistic. The D values calculated from the slope of the linear portion of these log – log plots are listed in Table 1. It can be seen from Table 1 that all the unsupported membranes have a rough surface with the fractal dimension less than that of SiO₂ membrane, ranging from 2.64 to 2.53. The roughness slightly decreases as the ZrO₂ /SiO₂ ratio increases. This is due to the pore formation mechanism of membranes.

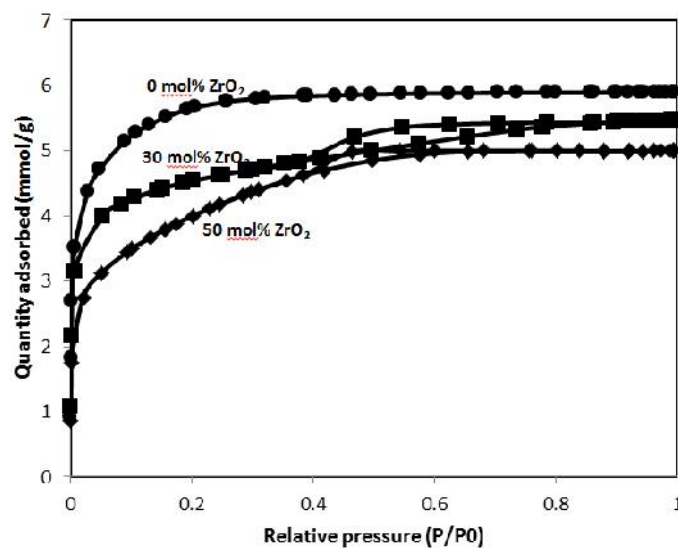


Fig. 5. N₂ adsorption-desorption isotherms silica containing different amounts of zirconia heat treated at 500 °C for 1 h.

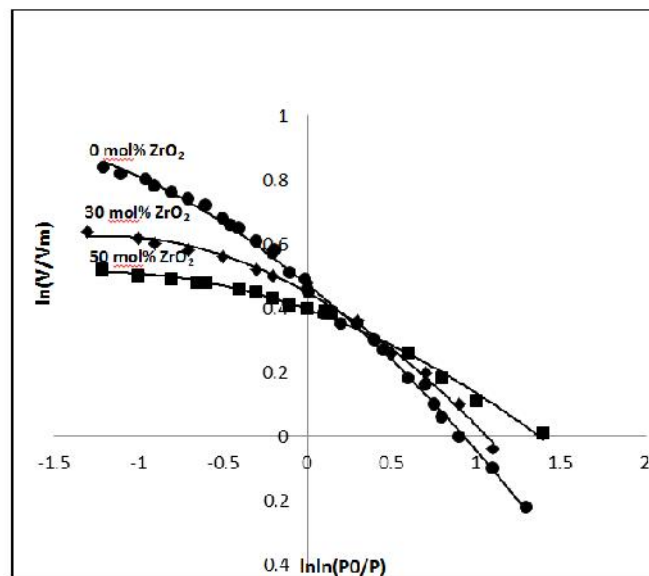
Table 1. Surface fractal dimension of SiO₂-ZrO₂ unsupported membranes with different amounts of zirconia at 500 °C for 1 h.

Membrane	D
SiO ₂	3
30 mol% ZrO ₂	2.64
50 mol% ZrO ₂	2.53

The pore network for zirconia is obtained by a packing of non-fractal particles [37], so the pores have a relatively smoother surface. In case the silica membrane is considered, for a wide range of processing conditions, polymeric silica sols characterized by a mass fractal dimension rather than non-fractal particulate sols are produced by hydrolysis and condensation of silicon alkoxides, and pore network results from the aggregation and interpenetration of individual silica fractal clusters [38]. It is reasonable that the pore will have a relatively rougher surface. As far as the composite membranes are concerned, the pore formation becomes rather complex because the porous network is controlled by both the particles packing and the polymeric clusters aggregation mechanism. The surface fractal dimension of pores depends on the amount, size and mass fractal dimension of polymeric clusters, as well as the extent to which the clusters interpenetrate. It is obvious that the more silica clusters are in the membrane, the greater the surface fractal dimension is, as shown in Table 1.

The isotherms of unsupported membrane with 30% ZrO₂ calcined from 200 to 500 °C are illustrated in Fig. 7. The calcined membranes have type IV-like isotherms. Fig. 8 shows the FHH plots of unsupported membrane heat treated at different temperature and the surface fractal dimensions are listed in Table 2. Table 2 reveals that the membrane remains rough on heating, and with increase of the heating temperature from 200 to 500 °C, the surface fractal dimension increases slightly to 2.64. When heating proceeds at 200 °C, most water and ethanol in the gel are vaporized.

The amorphous gels go through the so-called calcination step during which the organic additives continue to burn out when the temperature rises to 300 °C and some shrinkage occurs during heating at higher temperature (500 °C). Heating induces a restructuring phenomenon and results in the increase of the mass fractal dimension of silica clusters [39]; so, there is a slight increase of surface fractal dimension in the unsupported membrane.

**Fig. 6.** FHH plots for the SiO₂-ZrO₂ unsupported membranes with different amounts of zirconia at 500 °C for 1 h.

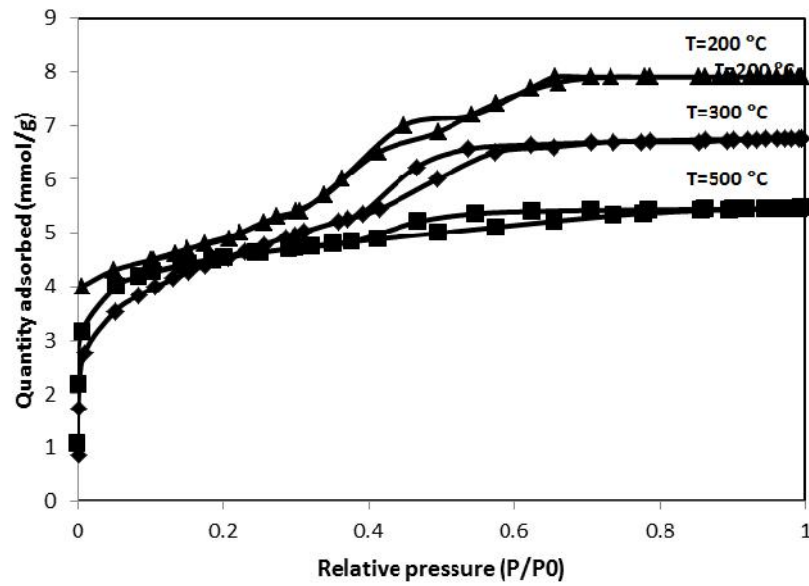


Fig. 7. N₂ adsorption-desorption isotherms on the silica unsupported membrane with 30 zirconia content heat treated at different temperatures for 1 h.

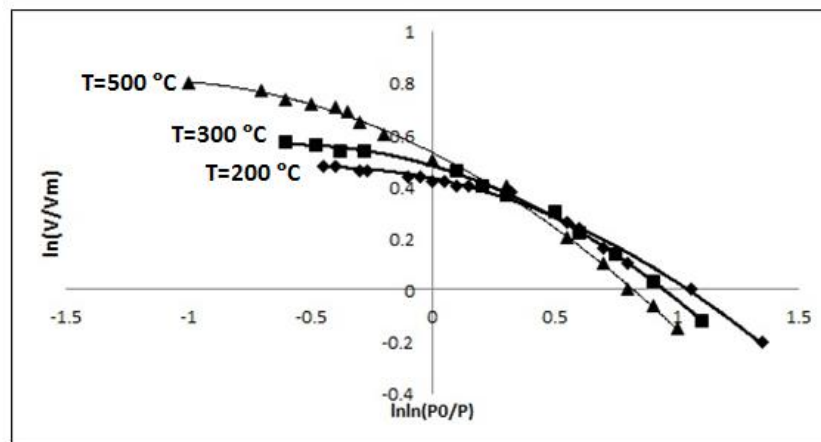


Fig. 8. FHH plots for the silica unsupported membrane with 30% zirconia heat treated at different temperatures for 1 h.

Table 2. Surface fractal dimension of silica unsupported membrane with 30% zirconia heat treated at different temperatures for 1 h.

Temperature	D
T=200 °C	2.51
T=300 °C	2.57
T=500 °C	2.64

3-2- characterization of supported membrane

FE-SEM image from the top view of SiO₂-30%ZrO₂ membrane is shown in Fig. 9.

As can be seen, no defect can be observed on the surface of the layer. In addition, the synthesized membrane has good surface uniformity.

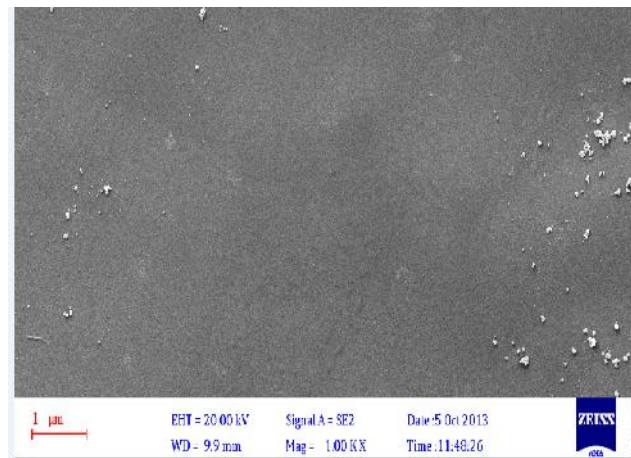


Fig. 9. FESEM image from surface of SiO₂-30%ZrO₂ membrane.

4. Conclusion

Dependence of surface fractal dimension of SiO₂-ZrO₂ unsupported membranes on chemical composition and heating temperature were studied in this paper. All unsupported membranes have rough surfaces and their fractal dimensions range from 2 to 3. Surface fractal dimension tends to decrease with the increase of ZrO₂ content in unsupported membrane. This feature is related to the porous texture which is determined by both the zirconia particles packing and silica polymeric clusters interpenetration and entanglement. According to BET analysis and surface fractal dimension, SiO₂-30%ZrO₂ membrane is suitable for gas separation. Heating induces a change of pore surface roughness. The surface fractal dimension first increases slightly when the heating temperature rises from 200 to 500 °C.

References

- [1] L. Wei, Z. Baoquan, L. Xiufeng, X. Liming, "Thermal stability of silica-zirconia membranes", *Chin. J. Chem. Eng.*, Vol. 14, 2006, pp. 31–36.
- [2] T. D. Chen, L. Wang, H. R. Chen, J. L. Shi, "Synthesis and microstructure of boron-doped alumina membranes prepared by sol-gel method", *Mater. Lett.*, Vol. 65, 2001, pp. 353–357.

- [3] R. Rodriguez, M. Estevez, S. Vargas, "photo-quenched of the luminescence signal in Co(II)-doped alumina prepared by the sol-gel method", *J. Non-Crys. Solids.*, Vol. 357, 2011, pp. 1383–1389.

- [4] C. A. Cooper, Y. S. Lin, "Microstructural and gas separation properties of CVD modified mesoporous -alumina membranes", *J. Member. Sci.*, Vol. 195, 2002, pp. 35–50.

- [5] Y. Farhang-Ghojeh Biglu, E. Taheri-Nassaj, "Synthesis and characterization of alumina supported sub-nanoporous SiO₂–10 wt% TiO₂ membrane for nitrogen separation", *Ind. Eng. Chem.*, Vol. 19, 2013, pp. 1752–1759.

- [6] C. Hobbs, S. Hong, J. Taylor, "Effect of surface roughness on fouling of RO and NF membranes during filtration of a high organic surficial groundwater", *J. Water. Supply. Res. Tech.*, Vol. 55, 2006, pp. 559–570.

- [7] S. Battersby, S. Smart, B. Ladewig, S. Liu, M. C. Duke, V. Rudolph, J. C. Diniz Da Costa, "Hydrothermal stability of cobalt silica membranes in a water gas shift membrane reactor", *Sep. Purif. Tech.*, Vol. 66, 2009, pp. 299–305.

- [8] T. Van Gestel, D. Sebold, F. Hauler, W. A. Meulenbergh, H. P. Buchkremer, "Potentialities of microporous membranes for H₂ /CO₂ separation in future fossil fuel power plants: evaluation of SiO₂, ZrO₂, Y₂O₃ –ZrO₂

- and TiO_2 – ZrO_2 sol–gel membranes”, *J. Member. Sci.*, Vol. 359, 2010, pp. 64–79.
- [9] V. Boffa, D. H. A. Blank, J. E. Elshof, “Hydrothermal stability of microporous silica and niobia silica membranes”, *J. Member. Sci.*, Vol. 319, 2008, pp. 256–263.
- [10] R. Igi, T. Yoshioka, Y. H. Ikuhara, Y. iwamoto, T. Tsuru, “Characterization of Co-doped silica for improved hydrothermal stability and application to hydrogen separation membranes at high temperatures”, *J. Am. Ceram. Soc.*, Vol. 91, 2008, pp. 2975–2981.
- [11] Y. Iwamoto, “Precursors-derived ceramic membranes for high-temperature separation of Hydrogen”, *J. Ceram. Soc. Jpn.*, Vol. 115, 2007, pp. 947–954.
- [12] M. Kanezashi, T. Fujita, M. Asaeda, “Nickel-doped silica membranes for separation of helium from organic gas mixtures”, *Sep. Sci. Tech.*, Vol. 40, 2005, pp. 225–228.
- [13] C. X. C. Lin, L. P. Ding, S. Smart, J. C. Diniz da Costa, “Cobalt oxide silica membranes for Desalination”, *J. Coll. Inter. Sci.*, Vol. 368, 2012, pp. 70–76.
- [14] D. Uhlmann, S. Smart, J. C. Diniz da Costa, “High temperature steam investigation of cobalt oxide silica membranes for gas separation”, *Sep. Purif. Tech.*, Vol. 76, 2010, pp. 171–178.
- [15] J. Yang, J. Chen, “Silver-doped organic-inorganic hybrid silica membranes by sol–gel method: preparation and hydrothermal stability”, *Sep. Sci. Tech.*, Vol. 46, 2011, pp. 2128–2137.
- [16] H. Lim, Y. Gu, S. T. Oyama, “Reaction of primary and secondary products in a membrane reactor: studies of ethanol steam reforming with a silica-alumina composite membrane”, *J. Member. Sci.*, Vol. 351, 2010, pp. 149–159.
- [17] M. Kanezashi, M. Asaeda, “Hydrogen permeation characteristics and stability of Ni-doped silica membranes in steam at high temperatures”, *J. Member. Sci.*, Vol. 271, 2006, pp. 86–93.
- [18] D. Uhlmann, S. Liu, B. P. Ladewig, J. C. Diniz da Costa, “Cobalt-oped silica membranes for gas Separation”, *J. Member. Sci.*, Vol. 326, 2009, pp. 316–321.
- [19] Y. Gu, S. T. Oyama, “Permeation properties and hydrothermal stability of silica-titania membranes supported on porous alumina substrates”, *J. Member. Sci.*, Vol. 345, 2009, pp. 267–275.
- [20] M. Asaeda, Y. Sakou, J. Yang, K. shimasaki, “Stability and performance of porous silica-zirconia composite membranes for pervaporation of aqueous organic solutions”, *J. Member. Sci.*, Vol. 209, 2002, pp. 163–175.
- [21] K. Yoshida, Y. Hirano, H. Fuji, T. Tsuru, M. Asaeda, “Hydrothermal stability and performance of silica–zirconia membranes for hydrogen separation in hydrothermal conditions”, *J. Chem. Eng. Jpn.*, Vol. 34, 2001, pp. 523–530.
- [22] H. Lio, L. Zhang, N. A. Seaton, “Further insights into the porous structure of TEOS derived silica gels”, *Langmuir.*, Vol. 9, 1993, p. 2576.
- [23] F. Rubio, J. Rubio, J. L. Oteo, “Preparation of nanometric titanium hydrous oxide particles by vapour phase hydrolysis of titanium tetrabutoxide”, *J. Sol– Gel. Sci. Tech.*, Vol. 8, 1997, p. 159.
- [24] D. Avnir, D. Farin, P. Pfeifer, “Molecular fractal surfaces”, *Nature.*, Vol. 308, 1984, p. 261.
- [25] Y. Lefebvre, S. Lacelle, C. Jolicoeur, “Surface fractal dimensions of some industrial minerals”, *J. Mater. Res.*, Vol. 7, 1992, p. 1888.
- [26] F. Ehrburger-Dolle, M. Holz, C. Mauzac, J. Lahaye, G. M. Pajonk, “Characterization of the porous texture of aerogels”, *J. Non-Cryst. Solids.*, Vol. 145, 1992, p. 185.
- [27] D. Avnir, M. Jaroniec, “Equilibria and Dynamics of Gas Adsorption on Heterogeneous Solid Surfaces”, *Langmuir.*, Vol. 5, 1989, p. 1431.
- [28] T. D. Chen, L. Wang, H. R. Chen, J. L. Shi, “Synthesis and microstructure of boron-doped alumina membranes prepared by sol–gel method”, *Mater. Let.*, Vol.65, 2001, pp. 353–357.
- [29] K. Yoshida, Y. Hirano, H. Fuji, T. Tsuru, M. Asaeda, “Hydrothermal stability and performance of silica–zirconia membranes for hydrogen separation in hydrothermal conditions”, *J. Chem. Eng. Jpn.*, Vol. 34, 2001, pp. 523–530.

- [30] M. Nocun, S. Siwulski, E. Leja, "Structural studies of TEOS-tetraethoxytitanate based hybrids", *Optic. Mat.*, Vol. 27, 2005, pp. 1523–1528.
- [31] X. Wu, X. Yao, M. Wang, L. Gao, "Effects of water content and sol viscosity on morphology of porous silica thermal insulating layer", *Ceram. Int.*, Vol. 30, 2004, pp. 1949–1951.
- [32] M. D. Zahir, K. Sato, H. Mori, Y. Iwamoto, "Preparation and properties of hydrothermally stable-alumina-based composite mesoporous membranes", *J. Am. Ceram. Soc.*, Vol. 89, 2006, pp. 2874–2880.
- [33] E. Pabon, J. Retuert, R. Quijada, A. Zarate, "Spectroscopic Properties of Inorganic and Organometallic Compounds", *J. Micro. Meso. Mat.*, Vol. 67, (2004), pp. 195–203.
- [34] C. Sanchez, J. Livage, M. Henry, "Chemical modification of alkoxide precursors", *J. Non. Crys. Solid.*, Vol. 10, 1988, pp. 65–76.
- [35] R. S. A. Lange, K. N. P. Kumar, J. H. A. Hekkink, "Microporous SiO_2 and SiO_2/MO_x ($M = \frac{1}{4}\text{Ti, Zr, Al}$) for ceramic membrane applications: a microstructural study of the sol-stage and the consolidated state", *J. Sol-Gel. Sci. Tech.*, Vol. 2, 1994, pp. 489–495.
- [36] A. F. M. Leenaars, K. Keier, A. J. Burggraaf, "Inorganic membranes synthesis, characteristics, and applications", *J. Colloid. Interface. Sci.*, Vol. 105, 1985, p. 27.
- [37] C. J. Brinker, R. Sehgal, S. L. Hietala, R. Deshpande, D. M. Smith, D. Loy, C. S. Ashley, "sol-gel strategies for amorphous, inorganic membranes exhibiting molecular sieving characteristics", *J. Member. Sci.*, Vol. 94, 1994, p. 85.
- [38] D.W. Schaefer, "Kinetics of Aggregation and Gelation", *Rev. Phys. Appl.*, Vol. 4, 1989, p. 121.
- [39] M. Mosquera, "Application of mercury porosimetry to the study of xerogels used as stone consolidants", *J. Non. Crys. Solid.*, Vol. 311, 2002, pp. 185–194.